

# Determination of Linke's Turbidity Factors from Model and Measure Solar Radiations in the Tropics Over Highland of South-East Ethiopia

Ambaye C

Madda Walabu University, Bale-Robe, Ethiopia

## Abstract

Linke's turbidity factors  $T_L$  and perceptible water vapor in the atmosphere are essential for evaluating pollution trends in the area. The rise of  $T_L$  is directly related to deforestation, industrialization, urbanization and influx of dusts and particulate matters from closer and far distance to the region. In this study, there is a computation of  $T_L$  from three methods global solar radiation (GSR) data. These are model, ground and satellite recorded GSR. The model codes of mathematical equations in determining model GSR and  $T_L$  were handled by MATLAB tool. The  $T_L$  from model GSR were compared with ground and satellite GSR in terms of statistical evaluation indicators: The coefficient of determination ( $R^2$ ), root mean squared error (RMSE), Nash-Sutcliffe efficiency (E), its relative efficiency criteria ( $E_r$ ), index agreement (d) and its relative efficiency criteria (dr). All  $T_L$ s from the model, ground and satellite GSR are approximately varied between 4 and 8. The rising levels have been approximately found in the range between 20% and 37.5% as compared to  $T_L$  of tropical warm air (continental) since 1947. Atmospheric turbidity is an important procedure for early warning on monitoring air, water, soil quality for stability of healthy ecosystem.

**Keywords:** Aerosols; Africa rising; Global solar radiation; Links turbidity factors; Perceptible water vapor

## Introduction

The attenuation of solar radiation through a real atmosphere *versus* that through a clean, dry atmosphere gives an indication of the atmospheric turbidity. It is a very suitable approximation to model the atmospheric absorption and scattering of the extraterrestrial radiation relative to dry and clean atmosphere [1]. Its study is important for monitoring atmospheric pollution through the presence of dust aerosols in the meteorology and climatology. Atmospheric turbidity associated with aerosols from dust loads, water vapor and anthropogenic source is also an important parameter for assessing pollution trends [2].

As other published literatures, atmospheric aerosol has increased enormously over the last two decades. It can either have non-anthropogenic or anthropogenic sources and are either emitted as primary particles (i.e. They are directly emitted to the atmosphere) or formed by secondary processes (i.e. By transformation of emitted precursor gases). It has been rising from low concentration over the preserved forest of Amazonian because of land-use change from natural begins to biomass burning [3] may bring  $T_L$  to the pollution level. According to Engelbrecht and Derbyshire [4] the pollution level of dust aerosols through the determination of  $T_L$  being closer to 8.

The global source regions of dust have covered the Northern Hemisphere, including North Africa, the Middle East, the Northwest Indian subcontinent, central Asia, and Northwest China [4]. Ethiopia is not immune from the large influx of dust because of its proximity, particularly in the Sahel and Arabia Peninsula. Influx dust from these regions, particulate matter from nearby industries, and smokes from deforestations for agriculture and fuel wood combined with maritime (Red Sea and Indian Ocean) moisture may contribute the rise of a turbidity factor in the area. The study area for this purpose is an Illusanbitu District located in tropical highland of South-East Ethiopia at about 7° latitude, 40° longitudes and 2500 m altitude. The determination of Linke's turbidity factor  $T_L$  was carried out from three method data.

- The meteorological data on Global Solar Radiation (GSR) were obtained from a non-government organization called Africa Rising [5] settled there.

- The model GSR data were extracted through integrating of mathematical equations from four atmospheric parameters by MATLAB tool.
- The satellite GSR data at the location was freely logged down from a website called Atmospheric Science Data Center controlled by the National Aeronautics and Space Administration NASA.

## Materials and Methods

### Mathematical formulations for global solar radiation modeling

The mathematical formulations were largely reviewed from the book written by Iqbal [6], and some published journals listed in the reference. The modeling in determining GSR entirely depends upon integrating the four major classifications of atmospheric parameters discussed below:

**a. Geographical Parameters:** The altitude and latitude in combining solar geometry climatic and optical parameters are essential in determining the amount of solar insolation reaching the earth's surface.

**b. Solar Geometric Parameters:** Under this category, the amount of solar irradiance reaching the study area are influenced by solar geometry parameters such the solar zenith angle  $\theta_z$ , declination angle  $\delta$  solar altitude angle  $\eta$  and solar hour angles  $\omega$ . The solar geometry called declination angle  $\delta$  is computed as:

$$\delta = 23.45 \sin\left(\frac{360}{365}(n + 284)\right) \quad (1)$$

**\*Corresponding author:** Ambaye C, Madda Walabu University, Bale-Robe, Ethiopia, Tel: +251911301844; E-mail: [janbo2012@gmail.com](mailto:janbo2012@gmail.com)

Received June 05, 2018; Accepted July 09, 2018; Published July 14, 2018

**Citation:** Ambaye C (2018) Determination of Linke's Turbidity Factors from Model and Measure Solar Radiations in the Tropics Over Highland of South-East Ethiopia. J Earth Sci Clim Change 9: 479. doi: [10.4172/2157-7617.1000479](https://doi.org/10.4172/2157-7617.1000479)

**Copyright:** © 2018 Ambaye C. This is an open-access article distributed under the terms of the Creative Commons Attribution License, which permits unrestricted use, distribution, and reproduction in any medium, provided the original author and source are credited.

The orientation of a horizontally placed solar receiver towards the incident radiation related to the declination angle  $\delta$ , solar zenith  $\theta_z$ , latitude  $\phi$ , solar altitude angle  $\eta$  and solar hour angle  $\omega$  in degree related as:

$$\sin \eta = \cos \theta_z = \sin \delta \sin \phi + \cos \delta \cos \phi \cos \omega \quad (2)$$

$$\omega = -15(LT-12) \quad (3)$$

Where  $L_t$  is the local time from the midnight. On the other hand, it is well known that atmospheric turbidities linked with the presence of aerosols, water vapor, and ozone are the most important extinction components affecting the direct and diffuse components of solar radiation under clear skies [7]. As a matter of fact, the effect of moist or water vapor is taken by considering the  $w$  in centimeter in terms, relative humidity  $H_r$ , ambient temperature  $T$  and partial pressure in Kelvin are expressed in Equations 4 and 5.

**a. Climatic parameters:** These classifications involve the measurement of ambient temperature, relative humidity, horizontal climate visibility and partial air pressure. The ambient temperature and relative humidity are also served for computing perceptible water vapor  $w$  using Equations 4 and 5. As a matter of fact, the effect of moist or water vapor is taken by considering the  $w$  in centimeter in terms, relative humidity,  $H_r$  ambient temperature  $T$  and partial pressure in Kelvin are expressed in these equations.

$$w = 0.49 \frac{H_r P_s}{T} \quad (4)$$

$$P_s = \exp\left(26.23 - \frac{5416}{T}\right) \quad (5)$$

The horizontal visibility  $V$  is also a significant climate factor in computing optical air transmittance in Equation (6). The horizontal Vis of the area lies within the range of 17 km up to 22 km during winter when there are low rainfall and cloud coverage.

**b. Atmospheric optical parameters:** It is the most complex atmospheric phenomena in determining the energy budget at a given location. The amount of solar energy reaching the surface is affected by optical properties of water vapor, air, ozone layer and aerosol masses. Their effects on solar irradiance are sensed by computing their optical transmittance, reflectance, absorbance, Rayleigh centeredness and turbidity coefficients that attenuate the solar irradiance reaching the surface. The ground albedo is also taken into consideration for modeling purposes. The computed value of relative optical masses of aerosol  $\tau_a$ , air mass  $m_a$ , water vapor  $m_w$  and ozone  $m_o$  at a given location are given under Equations (6), (7) (10) and (11) respectively. Their values are almost in closer ranges as stated by Iqbal [6]. However, an optical mass of aerosols  $m_o$  is the most uncertain parameters in calculating solar radiation on the ground [6]. They are highly variable in size, distribution, composition, and optical properties. For lack of required information, the value of computing optical air mass  $m_a$  can be used as a substitute for optical mass of aerosol  $m_o$  in Equation (7). Therefore, the optical transmittance  $\tau_a$  written in Eq. (6) as the presence of aerosols is calculated as

$$\tau_a = (0.97 - 1.265(V_{is})^{-0.66})^{m_a^{0.9}} \quad (6)$$

Where  $m_a$  is in the Equation (6) is the relative optical dry air mass for local conditions computed through Equations 7, 8, and 9.

$$m_a = m_r \frac{P}{P_o} \quad (7)$$

Where  $P$  and  $P_o$  are the local pressure and sea level pressures in millibars respectively. The local atmospheric pressure above sea level at altitude  $z$  is evaluated as:

$$\frac{P}{P_o} = \exp(-0.0001184z) \quad (8)$$

The altitude of the study location  $z$  is around 2480 m. The relative optical air mass  $m_r$  in Equation (7) may be approximated by relating to zenith angle  $\theta_z$ :

$$m_r = (\cos \theta_z + 0.15(93.885 - \theta_z)^{-1.253})^{-1} \quad (9)$$

On the other hand, the corresponding expressions for relative optical water vapor mass  $m_w$  and relative optical ozone mass  $m_o$  are expressed in the following two expressions by Iqbal.

$$m_w = (\cos \theta_z + 0.0584(92.650 - \theta_z)^{-1.452})^{-1} \quad (10)$$

$$m_o = \frac{1 + \frac{Z_3}{R_e}}{\left(\cos^2 \theta_z + 2 \left(\frac{Z_3}{R_e}\right)\right)^{\frac{1}{2}}} \quad (11)$$

Where  $Z_3$  measures the concentrated ozone at around 22 km and  $R_e$  is the radius of the earth approximated as 6370 km. Overall spectrally integrated transmittance computation for each atmospheric constituent is necessary steps for solar radiation parameterization in modeling [7]. The total transmittance  $\tau$  as a function of the ozone layer thickness  $\ell$  in cm, perceptible water vapor  $w$  in cm, turbidity coefficient  $\beta$  and  $\alpha$ , and the relative mass is evaluated by Iqbal [6]:

$$\tau = f(\ell, w, \beta, \alpha, m) \quad (12)$$

The transmittance quantities  $\tau_a$ ,  $\tau_o$  and  $\tau'_a$  for some major atmospheric constituents such as water vapors, ozone layers and aerosols are expressed as respectively in Equations (13), (16) and (28).

$$\tau_w = 1 - \alpha_w \quad (13)$$

Where  $\alpha_w$  is the attenuation coefficient of water vapor given as:

$$\alpha_w = \frac{2.9U_1}{(1 + 141.54)^{0.635} + 5.925U_1} \quad (14)$$

Where  $U_1$  is the pressure-corrected relative optical path length written in terms of  $m_r$  and  $w$  as:

$$U_1 = wm_r \quad (15)$$

The transmittance  $\tau_o$  due to the ozone layer is given as:

$$\tau_o = 1 - \alpha_o \quad (16)$$

Where  $\alpha_o$  is the attenuation coefficient due to direct irradiance transmission through the ozone layer. Its expression is written as:

$$\alpha_o = \frac{0.02118U_3}{1.0042U_3 + 3.23 \times 10^{-3}U_3^2} + \frac{1.082U_3}{(1 + 138.6U_3)^{0.805}} + \frac{0.0658U_3}{1 + (103.6U_3)^3} \quad (17)$$

The  $U_3$  is the ozone relative optical path given by:

$$U_3 = \ell m_r \quad (18)$$

For broad spectral range, the integrated transmittance for Rayleigh scattering  $\tau_r$  over the wavelength interval  $\Delta\lambda$  is defined as (Iqbal, 2012)

$$\tau_r = \frac{\left( \sum_{\lambda=0}^{\infty} I_{on} \exp(-0.008735\lambda^{-4.08} m_a) \Delta\lambda \right)}{I_{sc}} \quad (19)$$

$I_{on}$  is the direct irradiance on horizontal surface normal to the sun's rays (also called direct normal radiation) and  $I_{sc}$  is the solar constant whose value is 1367 W/m<sup>2</sup>. A regression-type correlation that fits Equation (19) is given as:

$$\tau_r = 0.972 - 0.08262m_a + 0.0093m_a^2 - 0.00095m_a^3 + 0.000437m_a^4 \quad (20)$$

During parameterization of the solar radiation, the direct normal irradiance  $I_{on}$  on a horizontal surface at a zenith angle  $\theta_z$  at mean sun-earth distance by including the correction factor called eccentricity  $\mathcal{E}$  can be given by Iqbal [6]:

$$I_{on} = \mathcal{E} I_{sc} (\tau_o \tau_r - \alpha_w) \tau_a \cos \theta_z \quad (21)$$

Where the eccentricity  $\mathcal{E}$  correction factor related to the number  $n$  of days in the year is given by:

$$\mathcal{E} = 1 + 0.033 \cos\left(\frac{360n}{365}\right) \quad (22)$$

Therefore, the total global irradiance  $I_T$  on a horizontal surface from direct irradiance and diffused irradiance  $I_d$  from surrounding environment can be written as follows:

$$I_T = I_{on} + I_d \quad (23)$$

The  $I_d$  can be further written as:

$$I_T = I_{dr} + I_{da} + I_{dm} \quad (24)$$

The broadband diffuse irradiance  $I_{dr}$  under a cloudless sky as the effect of Rayleigh scattering is given as

$$I_{dr} = I_{sc} \cos(\theta_z) \tau_o (0.5(1 - \tau_r)) \tau_a \quad (25)$$

On the other hand, the diffuse irradiance scattering because of aerosol-scattered diffuse radiation  $I_{da}$  reaching the ground after the first pass through the atmosphere is given as

$$I_{da} = I_{sc} \cos(\theta_z) (\tau_o \tau_r - \alpha_w) (F_c \omega_o (1 - \tau_o)) \quad (26)$$

Where  $F_c$  is symbolized for forward scattering,  $\omega_o$  is symbolized for the single scattering albedo by Iqbal, which is the ratio of energy scattered by aerosol to the total attenuation under primarily incident by the direct radiation. In this paper a value of  $F_c = 0.5$  [6] was taken for the computation. The determination of  $\omega_o$  is experimentally a troublesome, according to Iqbal [6]. However, a few amount of aerosol particles in rural environment usually scattered than those found in the urban-industrial area [6,8]. During solar irradiance modeling  $\omega_o = 0.6$ , by Iqbal [6] is used for urban-industrial region where as  $\omega_o = 0.9$  [6,8] is used for agricultural region. Since the study location is widely known as the rural and agricultural center, so  $\omega_o = 0.9$  was applied in the solar radiation modeling. The horizontal visibility ( $Vis$ ) for greater than 5 km, Ångström turbidity factor  $\beta$ , and wavelength exponent  $\alpha$  are related as:

$$\beta = 0.5^{-\alpha} (3.912 / Vis - 0.01162) \times (0.02472(Vis - 5) + 1.132) \quad (27)$$

The wavelength exponent  $\alpha = 1.3$  in Equations (27) and (28) was used in the computation according to Iqbal [6]. The aerosol transmittance  $\tau'_a$  computed using air-mass  $m'_a$ , Ångström turbidity factor  $\beta$ , and wavelength exponent  $\alpha$  is:

$$\tau'_a = (0.1245\alpha - 0.01162) + (1.003 - 0.125\alpha) \exp(-\beta m'_a (1.089\alpha + 0.5123)) \quad (28)$$

Where  $m'_a$  is the relative aerosol mass at the local station calculated

as:

$$m'_a = \frac{1.66P}{P_o} \quad (29)$$

The downward irradiance  $I_{dm}$  because of multiple reflections between the ground and the atmosphere is computed as:

$$I_{dm} = \left( I_{on} + I_{dr} + I_{da} \left( \frac{\rho_g \rho'_a}{1 - \rho_g \rho'_a} \right) \right) \quad (30)$$

Where  $\rho_g$  is the ground albedo and  $\rho'_a$  is cloudless sky albedo. The value of ground albedo for variation of multiply reflected irradiance lies between 0.2 and 0.7 according to Iqbal [6]. On another reference, the ground albedo varied between 0.1 and 0.25 for agricultural and grassland is written in Encyclopedia of Soil Science. In this paper  $\rho_g = 0.25$  was used for computing the downward irradiance  $I_{dm}$  due to multiple reflections between the ground and the atmosphere. The cloudless sky albedo  $\rho'_a$  is computed as Figures 1 and 2

$$\rho'_a = 0.0685 + 17(1 - \tau'_a) \omega_o \quad (31)$$

## Results and Discussion

Determination of linked turbidity factor  $T_L$

The influence of  $T_L$  on GSR at site were evaluated by Inman and Becker [9,10]:

$$T_L = (\delta_r m_a)^{-1} \ln \left( \frac{I_{sc}}{I_{on}} \right) \quad (32)$$

Where  $\delta_r$  is the Rayleigh optical thickness. It was employed in evaluating  $T_L$  were referenced by Inman [9]:

Its equation is represented as:

$$\delta_r = \frac{1}{9.4 + 0.94m_a} \quad (33)$$

$$T_L = \frac{\ln \left( \frac{I_{sc} \mathcal{E} \sin \eta}{I_{on}} \right)}{0.8662 \delta_r m_a} \quad (34)$$

The  $\delta_r$  is computed according the condition set by Wang, Chen, Niu, Salazar [11]. According to them  $\eta$  is to be greater than 10°,  $I_{on}$  is to be greater than 200 W/m<sup>2</sup> and the  $\delta_r$  is to be less than 20.

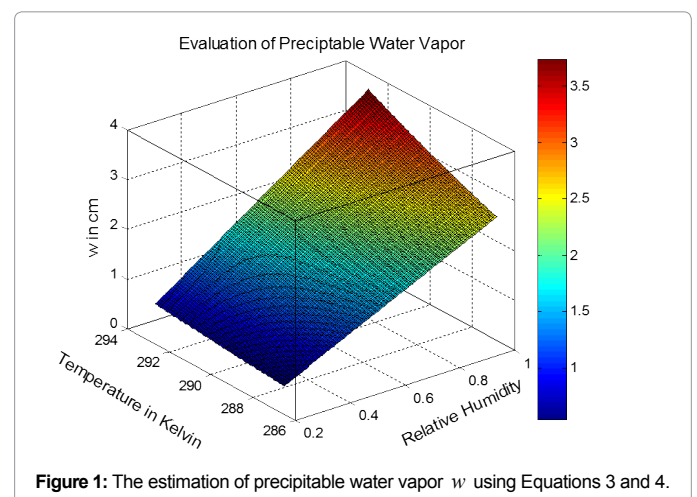


Figure 1: The estimation of precipitable water vapor  $w$  using Equations 3 and 4.

$$\delta_r = \frac{1}{6.577 + 1.1753m_a - 0.12002m_a^2 + 0.0665m_a^3 + 0.0013m_a^4} \quad (35)$$

The  $T_L$  illustrated on Figures 3-7 is from modeled GSR oscillated between 4.2 and 8.2 with its mean value about 6.2. The  $T_L$  from GSR of ground measurement is oscillated between 3.6 and 8.4 with mean value 6.16.

The statistical tools for evaluating hydrological model assessment widely discussed by Krause, Boyle, Bäse [12], where applicable for evaluating the model efficiency in determining  $T_L$ . These are: Root Means Squared Error RMSE, Nash-Sutcliffe efficiency  $E$  and its relative efficiency criteria  $E_r$ , index agreement  $d$  and its relative efficiency criteria  $d_r$  and coefficient of determination  $R^2$ .

An efficiency of 0 indicates that the model predictions are as

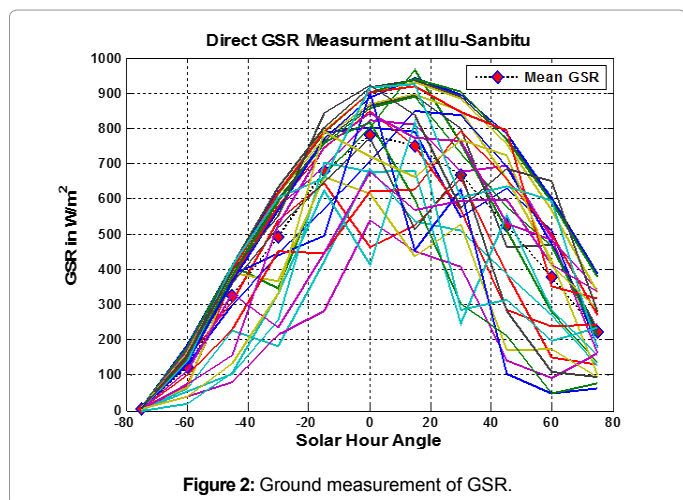


Figure 2: Ground measurement of GSR.

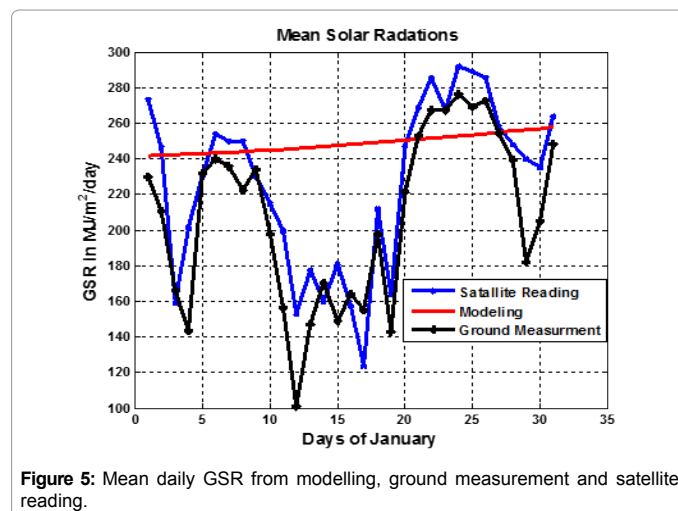


Figure 5: Mean daily GSR from modelling, ground measurement and satellite reading.

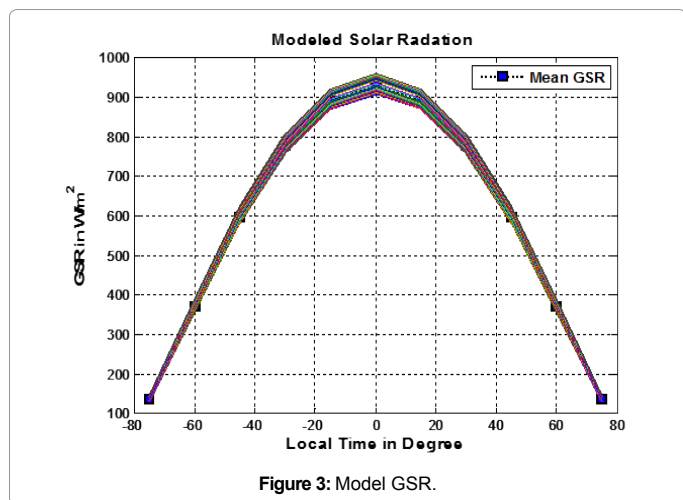


Figure 3: Model GSR.

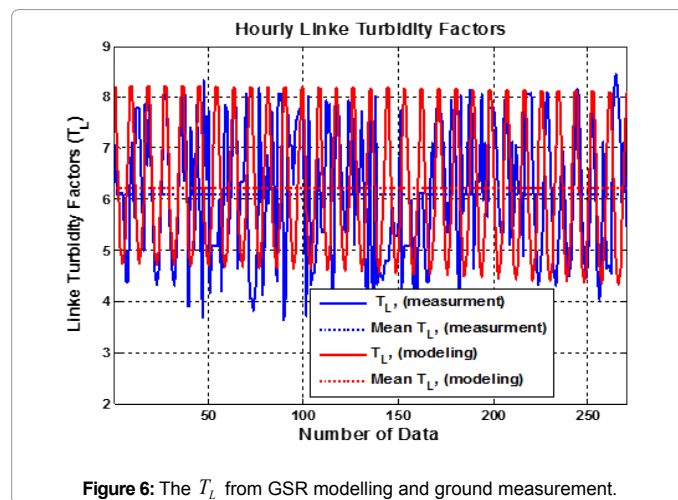


Figure 6: The  $T_L$  from GSR modelling and ground measurement.

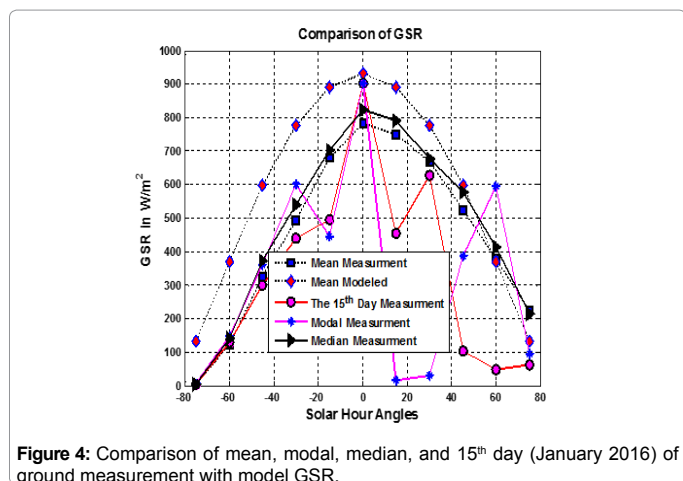


Figure 4: Comparison of mean, modal, median, and 15<sup>th</sup> day (January 2016) of ground measurement with model GSR.

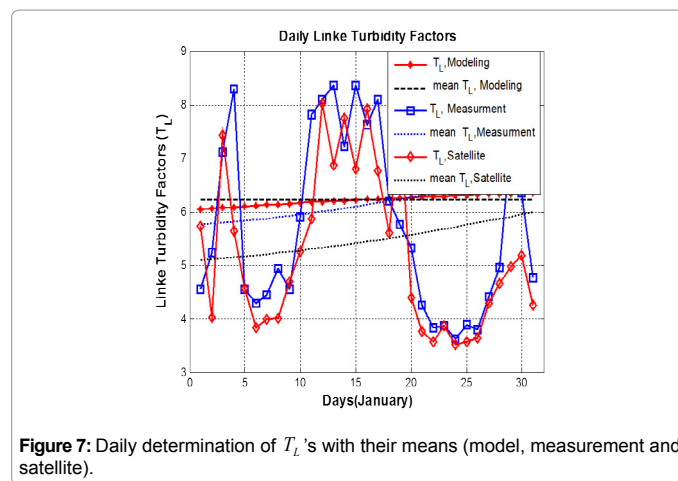


Figure 7: Daily determination of  $T_L$ 's with their means (model, measurement and satellite).

accurate as the mean of the observed data, whereas an efficiency less than zero ( $-\infty < E < 0$ ) occurs when the observed mean is a better predictor than the model. Essentially, the closer the model efficiency is to 1; the model is becoming more accurate. On the other statistical explanation on modeling, the coefficient of determination  $R^2$  ranging between 0.33 and 0.66 would have moderate explanatory power [13].

As it is seen in Figure 7 the daily  $T_L$  from model GSR is smoothly varied between 6.02 and 6.34 with mean 6.22. However, the daily  $T_L$  from ground GSR is considerably varied between 3.62 and 8.36 with the daily mean ranging between 5.77 and 6.71. The daily  $T_L$  from satellite GSR is also dramatically varied between 3.51 and 8.02 with daily mean lies between 5.12 and 6.01.

## Conclusion

The model GSR for the study is computed from integrated atmospheric parameters such as optical thickness, optical air mass, and ozone layer, the amount of aerosol effect, perceptible water vapor, climate data, solar geometry and geographical positions. This rise of Linke's turbidity factor is an outcome of the suspension of particulate matters, smokes and water droplet in the atmosphere. The area's proximity to Sahel and Arabia Peninsula, large influx of dusts can stream in to it. Maritime moisture from Red Sea and Indian Ocean combined with the dusts, particulate matters from local industries, smokes from traditional energy consumption patterns may bring the turbidity factors to the pollution level assisted through local and global wind system transport. These would have consistent pressure on the sustainability of water, air, and soil quality in the area. The  $T_L$  from the model, ground and satellite GSR is approximately in a close agreement varied between 4 and 8 with the daily average 6 point. This rise of  $T_L$  is approximately laid in the range between 20% to 37.5% as compared to  $T_L$  of tropical warm air (continental) in 1947 as discussed by Becker [10]. The result is almost in closer agreement with the analysis made in other continent (Asia) by Wang, Chen, Niu and Salazar [11], Computing the Linke's atmospheric turbidity is an important procedure for early warning on monitoring air, water, soil quality for stability of healthy ecosystem.

## Acknowledgments

The author appreciates and acknowledges heartily the teams in Africa Rising for providing meteorology data to academic researchers.

## References

1. Marif Y, Bechki D, Zerrouki M, Belhadj MM, Bouguettaia H (2017) Estimation of atmospheric turbidity over Adrar city in Algeria. Journal of King Saud 17: 1333-1317.
2. Abdelrahman MA, Said SAM, Shuaib AN (1988) Comparison between atmospheric turbidity coefficients of desert and temperate climates. Solar Energy 40: 219-225.
3. Fuzzi S, Baltensperger U, Carslaw K, Decesari S, Denier Van DGH (2015) Particulate matter, air quality and climate: Lessons learned and future needs. Atmospheric chemistry and physics 15: 8217-8299.
4. Engelbrecht JP, Derbyshire E (2010) Airborne mineral dust. Elements 6: 241-246.
5. Kemal SA (2017) Africa rising Ethiopia highlands final technical report January 2012 September 2016.
6. Iqbal M (2012) An introduction to solar radiation. Elsevier 2: 1.
7. Gueymard CA (2005) Importance of atmospheric turbidity and associated uncertainties in solar radiation and luminous efficacy modelling. Energy 30: 1603-1621.
8. Fraser RS, Kaufman YJ (1985) The relative importance of aerosol scattering and absorption in remote sensing. IEEE Transactions on Geoscience and Remote Sensing 5: 625-633.
9. Inman RH, Edson JG, Coimbra CF (2015) Impact of local broadband turbidity estimation on forecasting of clear sky direct normal irradiance. Solar Energy 117: 125-138.
10. Becker S (2001) Calculation of direct solar and diffuse radiation in Israel. International Journal of Climatology 21: 1561-1576.
11. Wang L, Chen Y, Niu Y, Salazar GA (2017) Analysis of atmospheric turbidity in clear skies at Wuhan, Central China. Journal of Earth Science 28: 729-738.
12. Krause P, Boyle DP, Båse F (2005) Comparison of different efficiency criteria for hydrological model assessment. Advances in geosciences 5: 89-97.
13. Huang CC, Wang YM, Wu TW, Wang PA (2013) An empirical analysis of the antecedents and performance consequences of using the moodle platform. International Journal of Information and Education Technology 3: 217.